Studying I-V Characteristic of an Optical Detector in Low Temperature

Bahareh Boroomandnasab[1], Abdolnabi kovsariyan[1], and Mohammad Sorosh[1]

[1]Electrical Department of Engineering Faculty Shahid Chamran University of Ahvaz, Iran,
B-Boroomand@mststu.scu.ir

Abstract: Optoelectronic devices in the range between LWIR and MWIR have several applications such as optical gas sensing, free-space optical communications, infrared measurement, thermal imaging and biomedical etc. Expression of applications, the need for research in the simulation of semiconductor detector features felt. HgCdTe semiconductor detector with a narrow band gap, which can range in wavelength of the aforementioned acts. It's possible to show an elements behavior and Performance by simulated without making it. So far, extensive research to reduce dark current and rise in device operation temperature is performed. Use at low temperatures will result in increased costs. The research was aimed to simulate a $Hg_{1-x}Cd_xTe$ light detector with considering tunneling effect, the Auger and SRH recombination. To achieve this goal, assist those equations to simulate drift - diffusion is done in MATLAB software.

[Boroomandnasab, B. , kovsariyan, A., and Sorosh, M., **Studying I-V Characteristic of an Optical Detector in Low Temperature.** *N Y Sci J* 2014;7(5):43-46]. (ISSN: 1554-0200). http://www.sciencepub.net/newyork. 9

Keywords: Optical detector, Simulation, Drift - Diffusion, Tunneling, recombination Auger, Recombination SRH

1 – Introduction

Infrared region is widely exclusive. To access the infrared wavelength region of narrow band materials have been investigated. Especially for this purpose, substances II - VI are provided great flexibility, because it can also as a wide band gap material, as well as narrow band gap material act. Properties of narrow-band HgCdTe, make it an important material for infrared detection. With its band gap tunnel leading to new hybrid devices, Also allows HgCdTe to have the features of both LWIR and MWIR. The most important challenge is that the device performs at low temperatures (Close to liquid nitrogen temperature) to achieve high efficiency.

2 - Numerical Modeling

A one-dimensional drift – diffusion model is used to simulate a homojunction $Hg_{1-x}Cd_xTe$ optical detector. Drift-diffusion simulations using a set of transport equations to describe the behavior of the device. Continuity equations for electrons and holes, the Poisson equation and all related recombination mechanisms are used. Poisson's equation for equilibrium is given by Equation 1.

$$\nabla^2.\varphi = -\frac{e}{\varepsilon}\left(n - p + N_D^{+} - N_A^{-}\right) \quad (1)$$

Where, ND^+ and NA^- are the ionized donor and acceptor concentrations and φ is the electrostatic potential. LU decomposition method is used for solving the Poisson equation. To calculate the current density equations 2 and 3 have been resolved.

$$J_n = -q\mu_n n\left(-\frac{d\varphi}{dx}\right) + qD_n\frac{dn}{dx} \quad (2)$$

$$J_p = -q\mu_p p\left(-\frac{d\varphi}{dx}\right) - qD_p\frac{dp}{dx} \quad (3)$$

where, $J_{n,p}$ is the current density, $\mu_{n,p}$ is the carrier mobility and $D_{n,p}$ is the diffusion coefficient. The diffusion coefficient for degenerate materials cannot simply be determined by the Einstein's relation and is therefore determined by Kroemer's expansion [1].

3- Theoretical Model

The mole fraction plays an important role in the determination of basic parameters such as band gap, intrinsic carrier concentration, effective mass, mobility and dielectric constant. These parameters are very sensitive to temperature [2].

a) The intrinsic carrier concentration

$$n_i = \left(5.585 - 3.820x + 1.753\times10^{-3}T - 1.364\times10^{-3}xT\right)\times E_g^{\frac{3}{4}}T^{\frac{3}{2}}e^{\left(-\frac{E_g}{2kT}\right)}\left(cm^{-3}\right) \quad (4)$$

In this equation "x" is cadmium mole fraction, T is the temperature and Eg is the band gap.

b) Band gap:

$$E_{(x,T)} = -0.302 + 1.93x + 5.35\times10^{-4}T(1-2x) - 0.810x^2 + 0.832x^3 \quad (5)$$

c) Effective mass:

$$m_n^* = \frac{1}{-0.6 + 6.333\left(\frac{2}{E_g} + \frac{1}{E_g + 1}\right)} \quad (6)$$

Hole mass m_p^* is equal to 0.55 m_0.

d) Electron and hole mobility:

e)

$$\mu_e = 9\times10^4\left(0.\frac{2}{x}\right)^7.5\,T^{-2\left(0.\frac{2}{x}\right)^6} \quad (7)$$

$$\mu_h = \frac{\mu_e}{100} \quad (8)$$

f) Electric permittivity:

$$\varepsilon_{HgCdTe} = 20.5 - 15.5x + 5.7x^2 \quad (9)$$

g) Absorption coefficient:

Two particular characterize the absorption coefficient, the Kane region, which describes the absorption for energies above the conduction band and the Urbach region, which describes the absorption for all energies below the conduction band edge [3].

$$\alpha = \beta\sqrt{E - E_g} \quad (10)$$

$$=\beta\text{-}1+0.083T+(21\text{-}0.13T)x \quad (11)$$

$$\alpha = \alpha_0 e^{\left(\frac{E-E_0}{T-T_0}\right)} \quad (12)$$

$$\alpha_0 = 3.267 \times 10^4(1+x) \quad (13)$$

$$E_0 = (1.838x) - 0.3424 \quad (14)$$

$$T_0 = 81.9 \quad (15)$$

h) recombination Mechanisms:

In this study, the mechanisms considered are Auger, SRH and radiant.

- SRH recombination is given by the following equation.

$$R_{SRH} = \frac{pn - n_i^2}{\tau_p\left[n + n_i e^{\left(\frac{E_T - E_i}{kT}\right)}\right] + \tau_n\left[p + n_i e^{\left(\frac{E_i - E_T}{kT}\right)}\right]} \quad (16)$$

where, 'E_t' is the trap level, 'Ei' is the intrinsic Fermi energy and '$\tau_{n,p}$' are the carrier lifetimes.

- Radiative recombination is a band to band recombination, including direct annihilation of a conduction electron band with the hole in the valence band. Additional energy generated, usually in the form of a photon will be free. This mechanism is a direct band gap material. Recombination Radiative given by the following equation.

$$R_{Radiative} = B(pn - n_i^2) \quad (17)$$

Where the B is given by the following equation.

$$B = (5.8 \times 10^{-13})\varepsilon^{\frac{1}{3}}\left(\frac{m_0}{m_e^* + m_h^*}\right)\left(1 + \frac{m_0}{m_e^*} + \frac{m_0}{m_h^*}\right)\left(\frac{300}{T}\right)^{\frac{3}{2}}(E_g^2 + 3kTE_g + 3.75k^2T^2) \quad (18)$$

Since $Hg_{1-x}Cd_xTe$ is a direct band gap material, expected to play a major role in recombination Radiative. Auger recombination is a one of the dominant mechanisms of a narrowband gap HgCdTe device. The Auger generation Usually is the Predominant parameter of dark current at high temperatures, that's why our photodetecor operates at near Liquid nitrogen temperature, But this will increase the operation cost. Auger generation-recombination is given by Equation 19.

$$R_{Auger} = C_n(pn^2 - nn_i^2) + C_p(np^2 - pn_i^2) \quad (19)$$

C_n and C_p are Auger coefficients. Which can be found in reference [4].

i) In a narrow band gap HgCdTe under reverse bias band to band tunneling is likely to increase with increasing reverse voltage that can be Estimate by WKB approximation [5].

$$G_T(x) = \frac{\sqrt{2}q^2\sqrt{m^*}F_x^2}{4\pi^2\hbar\sqrt{E_g}}\exp\left[\frac{-\pi\sqrt{m^*}E_g^{\frac{3}{2}}}{2\sqrt{2}q\hbar F_x}\right] \quad (20)$$

Where, G_T is expressed as a rate of tunneling and F_x is the local electric field.

j) When the trap band is in the middle of the band, trap level tunneling rises and with a high electric field can expect a large variance of the I-V diagram. The trap assisted tunneling can be expressed as a slight modification of equation 16 by adding a field effect factor 'Γn,p' [6].

$$R_{SRH} = \frac{pn - n_i^2}{\frac{\tau_p}{1+\Gamma_p}\left[n + n_i e^{\left(\frac{E_T - E_i}{kT}\right)}\right] + \frac{\tau_n}{1+\Gamma_n}\left[p + n_i e^{\left(\frac{E_i - E_T}{kT}\right)}\right]} \quad (21)$$

k) Dynamic resistance is an increasing resistance, which is measured by the following equation.

$$R_{Dynamic} = \left(\frac{dI}{dV}\right)^{-1} \quad (22)$$

4- Results

One of the important parts in the simulation of a semiconductor device is the spatial distribution of energy levels. Figure 1 shows the energy level diagram in equilibrium (no applied bias) and non-equilibrium (applied bias of 0.5 V), the general form of this distribution seems to be right, a depletion region is formed in the PN junction area. By applying a reverse bias the depletion region, the P and N height difference in energy level goes up, thus tunneling increases.

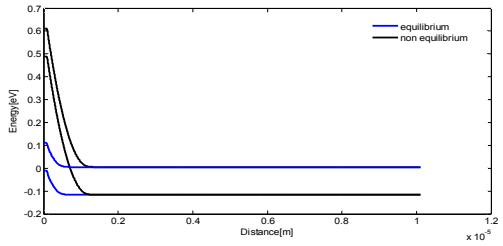

Figure 1: Diagram of the energy levels in both equilibrium and non-equilibrium for a $Hg_{1-x}Cd_xTe$ device with x = 0.225 at T = 78K. The length of the zone is P = 0.1 and n = 10.

Figure 2 shows the energy level diagram in equilibrium (no applied bias) and non-equilibrium (applied bias of 0.5 V) this diagram provides that, as expected, in a PIN structure, high injection does not affect the discharge area, that is why we can simultaneously have a large photosensitive area and a large electric field, which helps to separate the electron and hole pairs.

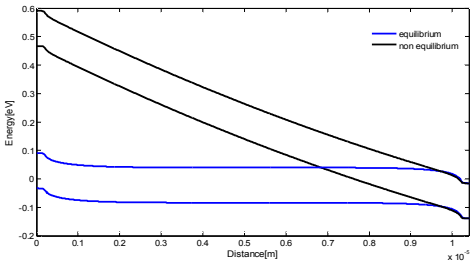

Figure 2: Diagram of the energy levels in both equilibrium and non-equilibrium for Hg1-xCdxTe device with x = 0.225 at T = 78K. The length of the zone is p = 0.2, n = 0.2 and I = 10 i.

In Figure 3 the dark current is shown in four different temperatures for a PN device. It is observed that the curves at 100K and 300K are similar to a diffusion controlled diode. This result is due to the energy gap reduces in the higher temperatures that increases the tunneling possibility.

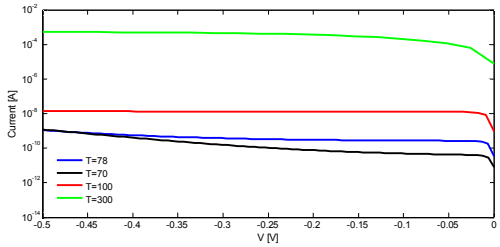

Figure 3: Dark current at four different temperatures for a PN device.

Figure 4 shows the dynamic resistance of a PN device. This value may be even extracted from $\left(\frac{dI}{dV}\right)^{-1}$ at V = 0. Peak area found between 0 to 0.1-V voltage is transition zone between diffusion and tunneling.

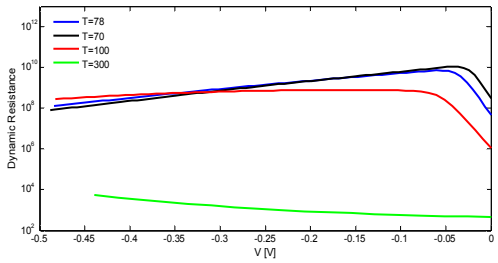

Figure 4: Dynamic Resistance against reverse voltage for a PN device.

Figure 5 shows the dark current at four different temperatures for a PIN device. It is observed that tunneling has a little effect on each I-V curve this is expected from the conduction band structure, the same as before increasing the temperature, increases dark current.

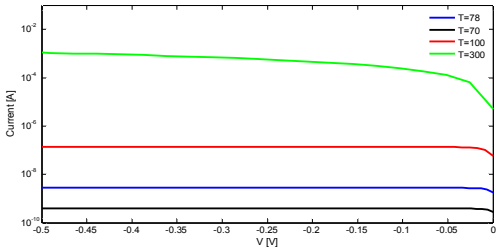

Figure 5: Dark current at four different temperatures for the PIN device.

In Figure 6 the dynamic resistance of a PIN device is shown. As seen the dynamic resistance of the device in negative voltages increased relative to the PN device but its sensitivity to temperature is higher, It is noteworthy that the dynamic resistance at zero voltage drop is higher than the PN detector. As expected peak of transition from tunneling to diffusion in Figure 5, does not exist.

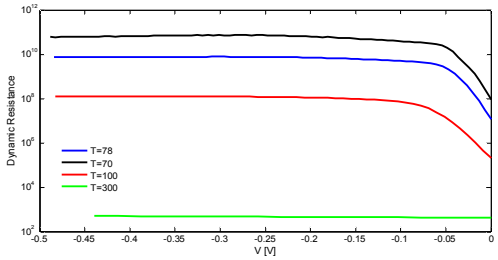

Figure 6: Dynamic Resistance against reverse voltage for the PIN device.

Reference

1. Kroemer, H. "The Einstein relation for degenerate carrier concentrations", IEEE Trans. Elec. Devices, vol. 25, no. 7, pp. 850, July 1978.
2. Srivastav, V., R. Pal, V. Venkataraman, "Performance study of high operating temperature HgCdTe mid wave infrared detector through numerical modelling", J. Appl. Phys. 108, 073112, 2010.
3. Chu, B. Li, J.H.,Y. Chang, Y.S. Gui, and D.Y. Tang, "Optical absorption above the energy band gap in Hg1-xCdxTe", Infrared Phys. 32,195, 1991.
4. Itsuno, A.M., J.D Phillips, S. Velicu, "Predicted performance improvement of Auger suppressed HgCdTe photodiodes and heterojunction detectors", IEEE Trans. Elec. Devices, vol.58, no.2, pp. 501-507, 2011.
5. Jozwikowski, K., M Kopytko, A. Rogalski, A. Jozwikowska, "Enhanced numerical analysis of current – voltage characteristics of long wavelength infrared n-on-p HgCdTe photodiodes", J. Appl. Phys., vol. 108, no. 7, 2010.
6. Hurkx, G.A.M, D.B.M Klassen, M.P.G Knuvers, F.G O'Hara, "A new recombination model describing heavy doping effects and low temperature behaviour", Proc. Int. Elec. Device Meeting, pp. 307-310, 1989.

5/6/2014